# Three-dimensional Rician Channel Characteristics in the Angular Domain

Derong Du, Xiaoping Zeng, Xin Jian, Feng Yu, Xiaoheng Tan, Xin Jiang, and Wei Fang

***Abstract*—The spatial selectivity of multipath fading channel impacts on the performance of the multiple antenna system. This paper investigates the three-dimensional (3-D) spatial selectivity of Rician channel in the angular domain to strive to alleviate the current lack of analytical studies. A 3-D model of the multipath angular power density (APD) for Rician channel is proposed. Then, the closed-form expressions of the 3-D unnormalized complex spherical harmonic coefficients and multipath shape factors are given based on the multipath APD using the theory of multipath shape factors. Finally, some important spatial fading statistics in the angular domain like the variance of the fading rate, spatial correlation, level crossing rate and minimum separation distance of antenna arrays are derived, and the impact of 3-D spatial angular directions on these spatial fading statistics is analyzed and simulated. The results provide useful insight on the analysis and design of the 3-D smart antenna arrays for the future fifth generation (5G) cellular networks.**

***Index Terms*—Three-dimensional spatial selectivity, Rician channel, multipath shape factors, angular power density**

## I. Introduction

The multiple antenna systems with the ability to improve spectral efficiency have become increasingly popular in recent years. The scatterers in the wireless communication environment produce the multipath components with distinct wave vectors, which results in the spatial selectivity [1]. The spatial selectivity of multipath fading impacts on the performance of the multiple antenna system. Many investigations on the channel spatial selectivity have been made in the Euclidean distance domain in various ways like analyzing and measuring the spatial correlation of multipath fading [2], [3]. However, there are few investigations on the channel spatial selectivity in the angular domain, which is absolutely essential for successful design of multiple antenna systems.

The theory of multipath shape factors can quantify and greatly simplify the description of multipath fading statistics of the non-omnidirectional channels in the angular domain. Many researchers have analyzed the spatial selectivity of multipath fading based on the theory, and these works can be traced back from two-dimensional (2-D) channels to three-dimensional (3-D) channels. In [4], the theory of multipath shape factors was proposed for the 2-D channel. According to the theory, the description of a 2-D multipath channel with arbitrary spatial complexity can be reduced to three shape factors (i.e., angular spread, angular constriction, and azimuthal direction of maximum fading) that have simple intuitive geometrical interpretations. The statistical analysis of Rician and Nakagami-m channels using the multipath shape factors was presented in [5] and [6]. Measurements of indoor angular profile were presented, and the angle-of-arrival (AoA) shape factors were derived at the millimeter wave band in [7] and [8]. Quantitative analysis of various spatial channel measurements and some scattering models using the multipath shape factors was presented in [9] and [10]. The shape factor of the angle spread was evaluated by comparing the different spatial/directional multipath characteristics in the urban and suburban scenarios in [11]. A geometric channel model to study the effect of antenna directivity on the angular power distribution at the mobile terminal was proposed in [12], and then the multipath shape factors were investigated to further exemplify the usefulness of the proposed model.

All previous investigations in [4]-[12] were made for 2-D multipath channels. However, 90% of the received power in urban measurements is contained in the paths with elevations up to 40° [13]. The measurement in [14] also shows that the mean elevations of the received power are from 1.8° for outdoor-indoor environments, up to 17.1° for urban macrocell environments. Those observations give a motivation for the analysis of the spatial selectivity for 3-D channels. A theory of 3-D multipath shape factors used to study the non-omnidirectional multipath channels was proposed in [15] in which the analytical expressions of the level crossing rate (LCR), average fade duration (AFD) and spatial correlation were derived for Rayleigh channels. In 3-D air-to-ground (A2G) radio propagation environments, the impact of various physical channel parameters (i.e., height of the air station, height of the base station and longest propagation path's delay) on the multipath shape factors defined in [4] was analyzed for the azimuth and elevation planes separately in [16].

The Rician fading is often used to describe the wireless multipath propagation with line-of-sight (LoS) and non-LoS (NLoS) components like A2G, air-to-air (A2A) [17] and

Manuscript received August 3, 2017; revised October 30, 2017. This work was funded by the National Natural Science Foundation of China (No. 61501065, No. 61571069, No. 61701054 and No. 61601067), the Fundamental Research Funds for the Central Universities (NO. 106112017 CDJQJ168817) and the Chongqing Research Program of Basic Research and Frontier Technology (No. CSTC2016JCYJA0021).

D. Du, X. Jian, F. Yu, and X. Tan are with the College of Communication Engineering, Chongqing University, Chongqing 400044, China (e-mail: {dr_du, jianxin, yufchn, txh}@cqu.edu.cn).

X. Jiang and W. Fang are with the Avionics Department of Beijing Aeronautical Science & Technology Research Institute (BASTRI), a branch center of Commercial Aircraft Corporation of China (COMAC), Beijing 102211, China (e-mail: {jiangxin2, fangwei1}@comac.cc).

X. Zeng is with the College of Communication Engineering, Chongqing University, Chongqing 400044, China (corresponding author, phone: +86-023-65111966; e-mail: zxp@cqu.edu.cn).

vehicle-to-vehicle (V2V) communications. However, as mentioned above, the 3-D spatial selectivity of Rician channel has been investigated rarely in the angular domain so far. This paper strives to alleviate the current lack of analytical studies by proposing a 3-D model of the multipath angular power density (APD). The closed-form expressions of the unnormalized complex spherical harmonic coefficients, multipath shape factors, variance of the fading rate, mean-squared time rate-of-change, spatial correlation, coherence distance, minimum separation distance of antenna arrays, LCR and AFD are given for the 3-D Rician channel. Finally, the analysis of the impact of 3-D spatial angular directions on these spatial fading statistics is presented through simulation. The results would provide useful insight on quantifying and greatly simplifying the analysis and design of the 3-D multiple input multiple output (MIMO) beamforming technology and smart antenna array for the future fifth generation (5G) cellular networks.

The remainder of the paper is organized as follows. Section II proposes a 3-D model of the multipath APD, unnormalized complex spherical harmonic coefficients, and the corresponding multipath shape factors of the Rician channel. Section III derives some important spatial fading statistics like the variance of the fading rate, spatial correlation and so on. Discussions on the obtained simulation results are provided in Section IV. Finally, conclusions are mentioned in Section V.

## II. 3-D Model of APD and Multipath Shape Factors

For the Rician channel in the densely populated built-up urban regions, it is assumed that the 3-D AoA [18] of the LoS component is $(\theta_0,\phi_0)$, and the 3-D AoA of the NLoS waves is $(\theta,\phi)$ which is uniformly distributed. Under the assumption that all the path gains of the NLoS waves have the same size, the 3-D multipath APD can be obtained as

$$\begin{aligned} p(\theta,\phi) &= P_{NLoS} f_{NLoS}(\theta,\phi) + P_{LoS} f_{LoS}(\theta,\phi) \\ &= \frac{P_T}{K+1} f_{NLoS}(\theta) f_{NLoS}(\phi) + \frac{P_T K}{K+1} f_{LoS}(\theta,\phi) \\ &= \frac{P_T}{K+1}\times\frac{1}{2\pi}\times\frac{1}{\pi} + \frac{P_T K \delta(\theta-\theta_0,\phi-\phi_0)}{K+1} \\ &= \frac{P_T}{2\pi^2(K+1)}\left[1+2\pi^2 K\delta(\theta-\theta_0,\phi-\phi_0)\right], \end{aligned} \tag{1}$$

where $P_T$ is the total received signal power in a local volume, $K$ is the Rician K-factor defined as the ratio of the power contributions by LoS path to the remaining multipaths, $P_{NLoS}=P_T/(K+1)$ is the power of the NLoS component, $P_{LoS}=P_T K/(K+1)$ is the power of the LoS component, $\theta_0,\theta\in[0,2\pi]$ are the azimuth angles, $\phi_0,\phi\in[-\pi/2,\pi/2]$ are the elevation angles, $f_{NLoS}(\theta,\phi)$ is the multipath APD of the NLoS component, and $\delta(\bullet,\bullet)$ is the 2-D Dirac delta function which is used to describe the multipath APD $f_{LoS}(\theta,\phi)$ of the LoS component.

According to the definition in [19], the $l$-th degree, $m$-th order unnormalized complex spherical harmonic coefficient $S_l^m$ for the multipath APD $p(\theta,\phi)$ in (1) can be derived, and the following six spherical harmonic coefficients which are used to obtain the 3-D multipath shape factors can be calculated as

$$\begin{aligned} S_0^0 &= \int_0^{2\pi}\int_{-\frac{\pi}{2}}^{\frac{\pi}{2}} p(\theta,\phi)\cos\phi\, d\phi\, d\theta = \frac{P_T}{\pi(K+1)}(2+\pi K\cos\phi_0) \\ S_1^0 &= \int_0^{2\pi}\int_{-\frac{\pi}{2}}^{\frac{\pi}{2}} p(\theta,\phi)\sin\phi\cos\phi\, d\phi\, d\theta = \frac{P_T K}{K+1}\sin\phi_0\cos\phi_0 \\ S_1^1 &= \int_0^{2\pi}\int_{-\frac{\pi}{2}}^{\frac{\pi}{2}} p(\theta,\phi)\cos^2\phi\exp(j\theta)\, d\phi\, d\theta \\ &= \frac{P_T K}{K+1}\cos^2\phi_0\exp(j\theta_0) \\ S_2^0 &= \int_0^{2\pi}\int_{-\frac{\pi}{2}}^{\frac{\pi}{2}} p(\theta,\phi)\left(\sin^2\phi-\frac{1}{3}\right)\cos\phi\, d\phi\, d\theta \\ &= \frac{P_T K}{K+1}\left(\sin^2\phi_0-\frac{1}{3}\right)\cos\phi_0 \\ S_2^1 &= \int_0^{2\pi}\int_{-\frac{\pi}{2}}^{\frac{\pi}{2}} p(\theta,\phi)\cos^2\phi\sin\phi\exp(j\theta)\, d\phi\, d\theta \\ &= \frac{P_T K}{K+1}\cos^2\phi_0\sin\phi_0\exp(j\theta_0) \\ S_2^2 &= \int_0^{2\pi}\int_{-\frac{\pi}{2}}^{\frac{\pi}{2}} p(\theta,\phi)\cos^3\phi\exp(j2\theta)\, d\phi\, d\theta \\ &= \frac{P_T K}{K+1}\cos^3\phi_0\exp(j2\theta_0). \end{aligned} \tag{2}$$

Therefore, the 3-D multipath shape factors defined in [15] to quantify and simplify the spatial fading statistics of the Rician channel can be derived as

$$\Lambda = \sqrt{1-\frac{(S_1^0)^2+|S_1^1|^2}{(S_0^0)^2}} = \frac{2\sqrt{1+\pi K\cos\phi_0}}{2+\pi K\cos\phi_0}, \tag{3}$$

$$\xi = \frac{\frac{3}{2}S_2^0 S_0^0-(S_1^0)^2+\frac{1}{2}|S_1^1|^2}{(S_0^0)^2-(S_1^0)^2-|S_1^1|^2} = \frac{\pi K\cos\phi_0\left(2-3\cos^2\phi_0\right)}{4(1+\pi K\cos\phi_0)}, \tag{4}$$

$$\chi = \frac{2|S_2^1 S_0^0-S_1^0 S_1^1|}{(S_0^0)^2-(S_1^0)^2-|S_1^1|^2} = \frac{\pi K\cos^2\phi_0|\sin\phi_0|}{1+\pi K\cos\phi_0}, \tag{5}$$

$$\gamma = \frac{\left|S_2^2 S_0^0-(S_1^1)^2\right|}{(S_0^0)^2-(S_1^0)^2-|S_1^1|^2} = \frac{\pi K\cos^3\phi_0}{2(1+\pi K\cos\phi_0)}, \tag{6}$$

$$\theta_{\phi 45}^{\max} = \arg\left\{S_2^1 S_0^0-S_1^0 S_1^1\right\} = \theta_0, \tag{7}$$

$$\theta_{\phi 0}^{\max} = \frac{1}{2}\arg\left\{S_2^2 S_0^0-(S_1^1)^2\right\} = \theta_0+\pi, \tag{8}$$

where $\Lambda$, $\xi$, $\chi$, $\gamma$, $\theta_{\phi 45}^{\max}$ and $\theta_{\phi 0}^{\max}$ are the 3-D angular spread, elevational constriction, 45°-inclined constriction, azimuthal constriction, azimuth of maximum fading at 45° elevation, and azimuth of maximum fading at zero elevation, respectively. The angular spread is a measure of how multipath waves concentrate about a single direction; the elevational constriction measures how much the multipath APD is concentrated on a single elevational cone or along two paths at same azimuth and opposite elevations; the 45°-inclined constriction measures how much the multipath APD is concentrated at the elevational angle 45°; the azimuthal

constriction measures how much the multipath power is concentrated on two paths on a single elevational cone.

## III. Spatial Fading Statistics

### A. Variance of the Fading Rate

The complex received voltage is one of the basic stochastic processes that are studied in a multipath fading analysis. The investigation of the position derivatives or rate-of-changes of the complex received voltage is useful to analyze how the complex received voltage changes over space. Since the mean derivative of a stationary process is zero, the variance of the fading rate of a received complex voltage is the simplest statistic that measures the fading rate. In a given direction, it is defined as the variance of its first derivative with respect to distance in that direction [15], and can be derived as

$$\sigma_{\dot{V}}^2(\theta,\phi)=\frac{4\pi^2\Lambda^2P_T}{3\lambda^2}\left\{1+\frac{3}{2}\left[\xi\left(2\sin^2\phi-\frac{2}{3}\right)+\chi\sin 2\phi\times\cos\left(\theta-\theta_{\phi 45}^{\max}\right)+\gamma\cos^2\phi\cos 2\left(\theta-\theta_{\phi 0}^{\max}\right)\right]\right\}, \tag{9}$$

where $\lambda$ is the carrier wavelength. By substituting (3)-(8) into (9), the variance of the fading rate of the 3-D Rician channel can be obtained.

For the mobile receiver, it is often convenient to measure the variance of the fading rate in terms of the change over time. According to [4], the mean-squared time rate-of-change of a received complex voltage can be written as

$$\sigma_{\dot{V}}^2(\theta,\phi)=\frac{4\pi^2\Lambda^2P_T\nu_R^2}{3\lambda^2}\left\{1+\frac{3}{2}\left[\xi\left(2\sin^2\phi-\frac{2}{3}\right)+\chi\sin 2\phi\times\cos\left(\theta-\theta_{\phi 45}^{\max}\right)+\gamma\cos^2\phi\cos 2\left(\theta-\theta_{\phi 0}^{\max}\right)\right]\right\}, \tag{10}$$

where $\nu_R$ is the velocity of the mobile receiver.

For direct comparison with Rayleigh models, (9) and (10) can be normalized by the variance of the fading rate of the 3-D Rayleigh channel. If $K$=0, then $\Lambda=1$, and $\xi=\chi=\gamma=0$ for Rayleigh fading, and the variance of the fading rate of the 3-D Rayleigh channel can be written as

$$\sigma_{\dot{V}\text{-}Ray}^2(\theta,\phi)=\frac{4\pi^2P_T}{3\lambda^2}. \tag{11}$$

Accordingly, the normalized variance of the fading rate and the normalized mean-squared time rate-of-change of a received complex voltage can be obtained by dividing (9) and (10) by (11), respectively.

### B. Spatial Correlation and Coherence Distance

In multiple antenna systems, the spatial correlation is a measure of the relationship between two antennas' signals. Multiple antenna channels are generally correlated due to low scattering and antenna array configurations. Correlated channels of the multiple antenna systems can reduce the high-capacity potential considerably, so the multiple antenna arrays should be designed with low or no correlation. The coherence distance is also one of the measures of the spatial selectivity of the wireless channel, and it is defined as the separation distance over which a fading channel appears to be unchanged. The signal envelopes which are sent or received by two antennas separated by the coherence distance experience practically uncorrelated fades.

The spatial correlation function of the 3-D Rician channel at a separation distance can be approximated by an arbitrary Gaussian function and its Mclaurin expansion [4], [20], i.e.

$$\begin{aligned}\rho_c(r,\theta,\phi)&=1-\frac{E\left[\left(\frac{dR}{dr}\right)^2\right]}{2\left\{E\left(R^2\right)-\left[E(R)\right]^2\right\}}\\&=1-\frac{\sigma_V^2}{2Var_{Ric}(R)}r^2+\cdots\approx\exp\left[-a\left(\frac{r}{\lambda}\right)^2\right]\\&\approx 1-a\left(\frac{r}{\lambda}\right)^2+\cdots.\end{aligned} \tag{12}$$

Accordingly,

$$a=\frac{\sigma_V^2\lambda^2}{2Var_{Ric}(R)}, \tag{13}$$

$$\begin{aligned}\rho_c(r,\theta,\phi)&\approx\exp\left[-\frac{\sigma_V^2r^2}{2Var_{Ric}(R)}\right]\\&=\exp\left\{\frac{-2(K+1)\sigma_V^2r^2}{P_T\left[4(K+1)-\pi\,{}_1F_1^2\left(-\frac{1}{2};1;-K\right)\right]}\right\},\end{aligned} \tag{14}$$

where $Var_{Ric}(R)$ is the variance of Rician distribution, ${}_1F_1(-1/2;1;-K)=\exp(-K/2)\left[(1+K)I_0(K/2)+KI_1(K/2)\right]$ is the confluent hypergeometric function of the first kind, $I_0(\bullet)$ is the zeroth order modified Bessel function of the first kind, and $I_1(\bullet)$ is the first order modified Bessel function of the first kind.

If the spatial correlation coefficient equals $\exp(-1)$ for the channel separable distance, the coherence distance can be derived as

$$D_c(\theta,\phi)=\frac{\sqrt{P_T\left[4(K+1)-\pi\,{}_1F_1^2\left(-\frac{1}{2};1;-K\right)\right]}}{\sigma_V\sqrt{2(K+1)}}. \tag{15}$$

### C. Minimum Separation Distance of Antenna Arrays

Multiple antenna arrays can bring huge spectral efficiency and radiated energy efficiency gains. Large scale antenna system has been selected as one of the main key technologies for the 5G cellular networks [21]. However, the available area where the antenna elements are placed is limited, and this makes the design of the separation distance between two adjacent antenna elements essential and challenging.

If the acceptable maximum of the spatial correlation can be described by $\rho_{\max}$ for antenna arrays, the separation distance $\Delta r$ between two adjacent antenna elements can be written as according to (14)

$$\Delta r=\frac{\sqrt{-2Var_{Ric}(R)\ln\rho_{\max}}}{\sigma_V(\theta,\phi)}. \tag{16}$$

Therefore, if $\sigma_V(\theta,\phi)$ is equal to its maximum, the minimum spacing $\Delta r_{\min}$ between two adjacent antenna

elements with the acceptable maximum of the spatial correlation can be obtained, i.e.

$$\begin{aligned}
&\max \sigma_V(\theta,\phi) \Leftrightarrow \max \sigma_V^2(\theta,\phi)\\
&\Leftrightarrow \max\left[\xi\left(2\sin^2\phi-\frac{2}{3}\right)+\chi\sin 2\phi\cos\left(\theta-\theta_{\phi 45}^{\max}\right)\right.\\
&\quad\left.+\gamma\cos^2\phi\cos 2\left(\theta-\theta_{\phi 0}^{\max}\right)\right]\\
&\Leftrightarrow \max\left[\xi\left(2\sin^2\phi-\frac{2}{3}\right)+\chi\sin 2\phi+\gamma\cos^2\phi\right]\\
&\quad=\max\left[\left(\frac{\gamma}{2}-\xi\right)\cos 2\phi+\chi\sin 2\phi+\frac{\gamma}{2}+\frac{\xi}{3}\right],\\
&\quad\theta=\theta_{\phi 0}^{\max}=\theta_{\phi 45}^{\max}\\
&\Leftrightarrow \max\left[\left(\frac{\gamma}{2}-\xi\right)\cos 2\phi+\chi\sin 2\phi\right]\\
&\quad=\max\left[\sqrt{\chi^2+\left(\frac{\gamma}{2}-\xi\right)^2}\sin(2\phi+\varphi)\right],\\
&\quad\varphi=\arcsin\frac{\gamma-2\xi}{\sqrt{4\chi^2+(\gamma-2\xi)^2}},\theta=\theta_{\phi 0}^{\max}=\theta_{\phi 45}^{\max}\\
&\Leftrightarrow \phi=\frac{\pi-2\varphi}{4},\varphi=\arcsin\frac{\gamma-2\xi}{\sqrt{4\chi^2+(\gamma-2\xi)^2}},\\
&\quad\theta=\theta_{\phi 0}^{\max}=\theta_{\phi 45}^{\max}.
\end{aligned} \tag{17}$$

Accordingly,

$$\begin{aligned}
\Delta r_{\min}&=\frac{\sqrt{-2Var_{Ric}(R)\ln\rho_{\max}}}{\max\sigma_V(\theta,\phi)}\\
&=\frac{\sqrt{-2Var_{Ric}(R)\ln\rho_{\max}}}{\frac{\pi\Lambda}{\lambda}\sqrt{\frac{P_T}{3}\left[4+3\sqrt{4\chi^2+(\gamma-2\xi)^2}+3\gamma+2\xi\right]}}\\
&=\frac{\lambda}{\pi\Lambda}\sqrt{\frac{-3\left[4(K+1)-\pi_1F_1^2\left(-\frac{1}{2};1;-K\right)\right]\ln\rho_{\max}}{2(K+1)\left[4+3\sqrt{4\chi^2+(\gamma-2\xi)^2}+3\gamma+2\xi\right]}}.
\end{aligned} \tag{18}$$

### D. Level Crossing Rate and Average Fade Duration

The LCR is defined as the average number of crossings per unit distance that the process drops beneath a specified threshold level. It is a measure of the fading rate and can be written as

$$\begin{aligned}
N(\rho_N,\theta,\phi)&=\int_0^\infty \dot r p(\rho_N,\dot r)d\dot r=p(\rho_N)\int_0^\infty p(\dot r)\dot r d\dot r\\
&=p(\rho_N)\int_0^\infty\sqrt{\frac{1}{2\pi\sigma_V^2}}\exp\left(-\frac{\dot r^2}{2\sigma_V^2}\right)\dot r d\dot r\\
&=\frac{\sqrt{2\pi}\sigma_V}{2\pi}p(\rho_N)\\
&=\frac{\sqrt{2\pi}\sigma_V\rho_N}{2\pi\sigma^2}\exp\left(-\frac{\rho_N{}^2+\rho^2}{2\sigma^2}\right)I_0\left(\frac{\rho_N\rho}{\sigma^2}\right),
\end{aligned} \tag{19}$$

where $\rho_N=R_l/\sqrt{P_T}$ is the normalized threshold level, $R_l$ is the envelope threshold, $p(\rho_N,\dot r)$ is the joint probability density function (PDF) of Rician envelope and its time derivative, $p(\rho_N)$ is the PDF of Rician envelope, $p(\dot r)$ is the PDF of the derivative of Rician envelope [22], $\rho=\sqrt{P_{LoS}}$, and $\sigma=\sqrt{P_{NLoS}/2}$.

The AFD is the duration that the signal spends below the threshold level and can be formulated as

$$\begin{aligned}
\bar l(\rho_N,\theta,\phi)&=\frac{1}{N(\rho_N,\theta,\phi)}\int_0^{\rho_N}p(r)dr\\
&=\frac{1}{N(\rho_N,\theta,\phi)}\left[1-Q_1\left(\frac{\rho}{\sigma},\frac{r}{\sigma}\right)\right]_0^{\rho_N}\\
&=\frac{Q_1\left(\frac{\rho}{\sigma},0\right)-Q_1\left(\frac{\rho}{\sigma},\frac{\rho_N}{\sigma}\right)}{N(\rho_N,\theta,\phi)},
\end{aligned} \tag{20}$$

where $Q_1(\bullet)$ is the Marcum Q-function.

## IV. Results and Discussions

This section demonstrates and analyses the multipath shape factors, variance of the fading rate of a complex voltage, LCR, AFD, spatial correlation, coherence distance and minimum separation distance of antenna arrays described in sections II and III for the 3-D Rician channel in the angular domain. Unless indicated otherwise, the channel parameters used to obtain the simulation curves are set to $\lambda=0.125$ m, $K=2$ dB, $P_T=1$, $\theta_0=\pi/4$, and $\phi_0=\pi/6$ for the urban communication scenarios.

### A. Multipath Shape Factors

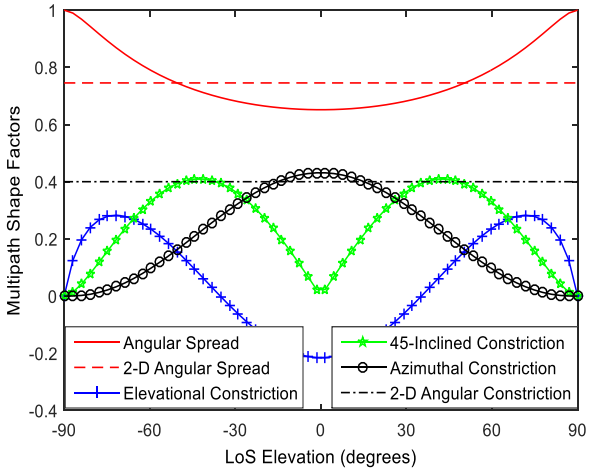


Fig. 1. The 2-D and 3-D multipath shape factors.

Fig. 1 demonstrates the 3-D multipath shape factors in (3)-(6) and the 2-D multipath shape factors in [4] for different elevation angles $\phi_0$ of LoS. As shown in Fig. 1, the 2-D multipath shape factors are constants and independent of the 3-D spatial angular directions. However, as mentioned in section I, the received signal power in urban measurements is distributed in the 3-D space [13], [14]. Therefore, the 2-D multipath shape factors cannot fully characterize the spatial selectivity of the Rician channels. This indicates the disadvantage of the 2-D channel model. Fig. 1 shows that all the 3-D multipath shape factors curves are symmetric about the elevation angle $\phi_0=0$. Besides, the angular spread $\Lambda$, elevational constriction $\xi$ and 45°-inclined constriction $\chi$ have their minimums at $\phi_0=0$, and on the contrary, the

azimuthal constriction $\gamma$ has a maximum. Furthermore, the angular spread $\Lambda = 1$ at $\phi_0 = \pm\pi/2$ denotes no clear bias in the direction of the multipath APD, and the minimum of $\Lambda$ at $\phi_0 = 0$ denotes the multipath APD relatively concentrates about a single direction; the elevational constriction $\xi = -0.5$ denotes a multipath APD distribution on a single elevational cone, and $\xi = 1$ denotes exactly two paths incoming from opposite elevations. Thus, the elevational constriction in Fig. 1 denotes the intermediate state; the 45°-inclined constriction $\chi = 0$ at $\phi_0 = 0, \pm\pi/2$ denotes a horizontal and/or vertical mirror symmetry of the multipath APD; the azimuthal constriction $\gamma = 0$ at $\phi_0 = \pm\pi/2$ denotes no clear bias in two arrival directions. Therefore, fading behaviors of the multipath shape factors mainly depend on the AoA of the LoS wave, and the 3-D multipath shape factors can capture the angular information of the Rician channels well.

### *B. Variance of the Fading Rate, Level Crossing Rate and Average Fade Duration*

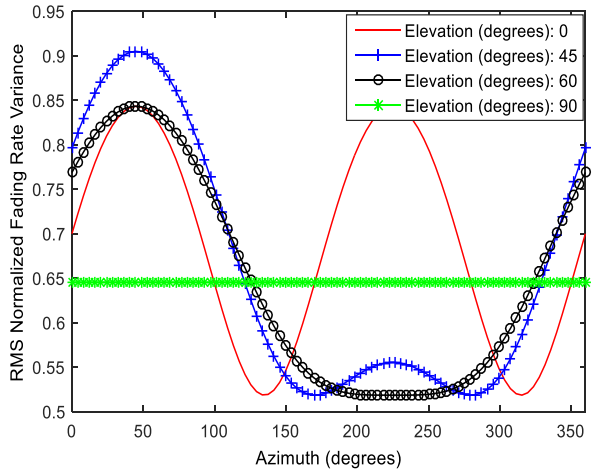


Fig. 2. The 3-D RMS normalized variance of the fading rate.

Fig. 2 demonstrates the 3-D root mean square (RMS) normalized variance of the fading rate in (9) for different directions $(\theta,\phi)$. Since the elevation angle of LoS is set to $\theta_0 = \pi/4$, the azimuth of maximum fading at 45° elevation and the azimuth of maximum fading at zero elevation are $\theta_{\phi 45}^{\max} = \pi/4$ and $\theta_{\phi 0}^{\max} = 5\pi/4$, respectively. Therefore, as shown in Fig. 2, RMS normalized variance of the fading rate curves with the elevation angles of $\pi/4$ and 0 have their maximums at the azimuth angles of $\pi/4$ and $5\pi/4$, respectively. The antenna array should be pointed away from the directions $(5\pi/4, 0)$ and $(\pi/4, \pi/4)$ in wireless communications, because the Rician channel fades fastest in the two directions. In addition, RMS normalized variance of the fading rate with the elevation angle of $\pi/2$ is a constant denoting its independence of the horizontal plane. As shown in Fig. 2, RMS normalized variances of the fading rate are less than 1, which implies that the Rayleigh channel fades faster than the Rician channel in the 3-D space. Since the mean-squared time rate-of-change of a received complex voltage $\sigma_{\dot{V}}^2(\theta,\phi)$ is equal to the variance of the fading rate $\sigma_{\dot{V}}^2(\theta,\phi)$ multiplied by the squared velocity of the receiver, $\sigma_{\dot{V}}^2(\theta,\phi)$ has the same characteristics as in Fig. 2. From Figs. 1 and 2, we note that the 3-D AoA direction of received signal waves has significant effect on the multipath shape factors and RMS normalized variance of the fading rate. According to (9), (11), (19) and (20), the LCR with a certain threshold is directly proportional to the RMS normalized variance of the fading rate, and the AFD is inversely proportional to the LCR. Therefore, dynamic behaviors in the angular domain of the LCR and AFD can be inferred from Fig. 2.

### *C. Spatial Correlation and Coherence Distance*

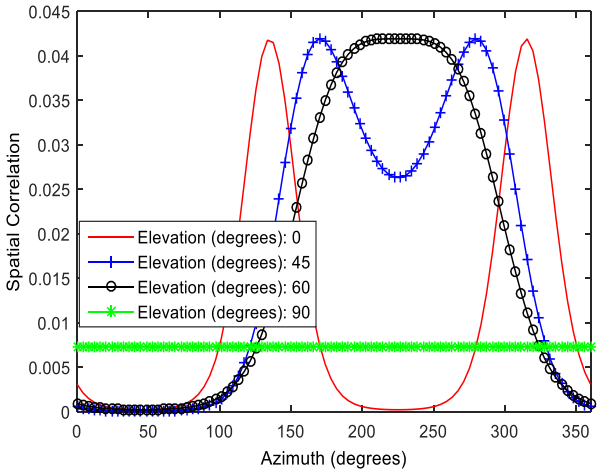


Fig. 3. The 3-D spatial correlation.

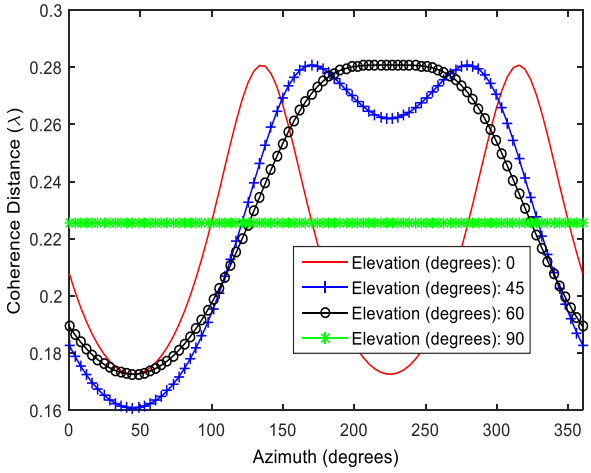


Fig. 4. The 3-D coherence distance.

Fig. 3 demonstrates the 3-D spatial correlation described by (14) for different directions $(\theta,\phi)$ with the separation distance $r = \lambda/2$. As shown in Fig. 3, the spatial correlation curves with different elevation angles have different varying patterns. Furthermore, the curve with the elevation angle of $\pi/2$ is also a straight line, implying a constant spatial correlation in the horizontal plane, but it varies greatly in the other directions. The curves of the spatial correlation with the elevation angles of 0, $\pi/4$ and $\pi/3$ have their minimums at the azimuth angle of $\theta = \pi/4$. Therefore, the 3-D spatial correlation is sensitive to the directions $(\theta,\phi)$, and this is valuable to the 3-D MIMO beamforming technology and the design of multiple antenna array. Moreover, the 3-D spatial

correlations in Fig. 3 are very small denoting that $\lambda/2$ is the proper separation distance between two adjacent antenna elements in urban communication scenarios. Fig. 4 demonstrates the 3-D coherence distance described by (15) for different directions $(\theta,\phi)$ with the spatial correlation coefficient $\exp(-1)$. As shown in Fig. 4, the coherence distance curves have the similar varying patterns as the spatial correlations in Fig. 3. The coherence distance provides a measure of the needed separation for a multiple antenna system. The explicit angular dependence of the coherence distance suggests that different separation distances in different 3-D spatial directions may be needed for the multiple antenna system employing the spatial diversity [23]. As shown in Figs. 3 and 4, the spatial correlation and coherence distance have their minimums at $(5\pi/4,0)$ and $(\pi/4,\pi/4)$, because the Rician channel fades fastest in the two directions.

### D. Minimum Separation Distance of Antenna Arrays

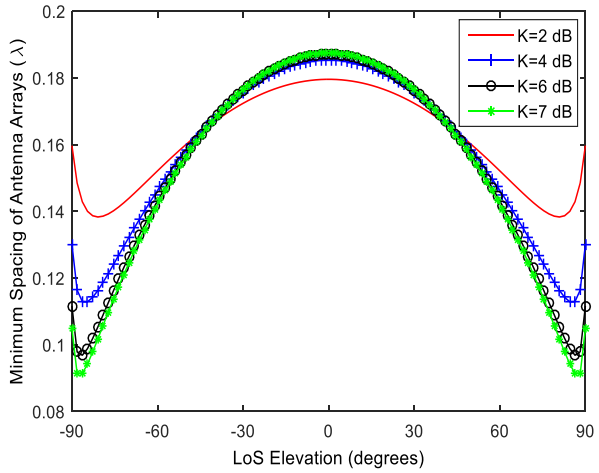


Fig. 5. The minimum separation distance of antenna arrays.

Fig. 5 demonstrates the minimum separation distance of antenna arrays described by (18) for different elevation angles $\phi_0$ of LoS and Rician K-factors with the acceptable maximum of the spatial correlation $\rho_{\max} = 0.3$. As shown in Fig. 5, the curves of the minimum separation distances of antenna arrays are symmetric about the elevation angle $\phi_0 = 0$, and they have their maximums at $\phi_0 = 0$. Furthermore, the larger the K-factor is, the larger the maximums of the curves. Meanwhile, we also notice that the curves of the minimum separation distance are almost overlapping if the K-factors are not less than 6 dB. To reduce the impact of the spatial correlation, the minimum separation distance between adjacent antenna elements is suggested to be more than $0.19\lambda$ for the antenna array designed in urban communication scenarios. According to (14), (15), (18) and Figs. 3-5, the theory of 3-D multipath shape factors can quantify and greatly simplify the analysis and design of the multiple antenna arrays.

## V. Conclusion

In this paper, a 3-D model of the multipath APD has been proposed to analyze the spatial selectivity of the Rician channel in the angular domain. The closed-form expressions of the 3-D unnormalized complex spherical harmonic coefficients, multipath shape factors, variance of the fading rate, mean-squared time rate-of-change, spatial correlation, coherence distance, minimum separation distance of antenna arrays, LCR and AFD have been derived. The simulation analysis shows that the 3-D spatial angular directions have significant effect on these fading statistics of the Rician channel. The results would provide useful insight on quantifying and greatly simplifying the analysis and design of the 3-D MIMO beamforming technology and smart antenna arrays for the future 5G cellular networks.

## References

[1] L. Pang, Y. Zhang, J. Li, X. Liang, Q. Wang, and X Liu, "Channel Correlation Analysis by Exploiting Temporal-Spectral-Spatial Information," *Chinese Journal of Electronics*, vol. 24, no. 2, pp. 379-387, Apr 2015:

[2] W. Q. Malik, "Spatial correlation in ultrawideband channels," *IEEE Transactions on Wireless Communications*, vol. 7, no. 2, pp. 604-610, Feb 2008.

[3] Z. Li, F. Luan, Y. Zhang, L. Xiao, L. Huang, S. Zhou, X. Xu, and J. Wang, "Capacity and spatial correlation measurements for wideband distributed MIMO channel in aircraft cabin environment," in *Proc. 2012 IEEE Wireless Communications and Networking Conference (WCNC)*, Shanghai, 2012: 1175-1179.

[4] G. D. Durgin and T. S. Rappaport, "Theory of multipath shape factors for small-scale fading wireless channels," *IEEE Transactions on Antennas and Propagation*, vol. 48, no. 5, pp. 682–693, May 2000.

[5] J. Lu and Y. Han, "Application of multipath shape factors in Nakagami-m fading channel," in *Proc. IEEE International Conference on Wireless Communications & Signal Processing*, 2009: 1-4.

[6] H. Shang, Y. Han, and J. Lu, "Statistical analysis of Rician and Nakagami-m fading channel using multipath Shape factors," in *Proc. IEEE International Conference on Computational Intelligence and Natural Computing Proceedings (CINC)*, 2010: 398-401.

[7] N. Moraitis, P. Constantinou, and D. Vouyioukas, "Power angle profile measurements and capacity evaluation of a SIMO system at 60 GHz," in *Proc. 21st Annual IEEE International Symposium on Personal, Indoor and Mobile Radio Communications*, 2010: 1027-1031.

[8] N. Moraitis, D. Vouyioukas, and P. Constantinou, "Indoor angular profile measurements and channel characterization at the millimeter-wave band," in *Proc. IEEE 5th European Conference on Antennas and Propagation (EUCAP)*, 2011: 155-159.

[9] Z. M. Loni, R. Ullah, and N. M. Khan, "Analysis of fading statistics based on angle of arrival measurements," in *Proc. IEEE 2011 International Workshop on Antenna Technology (iWAT)*, 2011: 314-319.

[10] Z. M. Loni and N. M. Khan, "Analysis of fading statistics in cellular mobile communication systems," *The Journal of Supercomputing*, vol. 64, no. 2, pp.295-309, May 2013.

[11] I. Rodriguez, E. P. L. Almeida, R. Abreu, M. Lauridsen, A. Loureiro, and P. Mogensen, "Analysis and comparison of 24 GHz cmWave radio propagation in urban and suburban scenarios," in *Proc. IEEE Wireless Communications and Networking Conference (WCNC)*, 2016: 1-7.

[12] Y. Chen, Z. Zhang, and V. K. Dubey, "Effect of antenna directivity on angular power distribution at mobile terminal in urban macrocells: A geometric channel modeling approach," *Wireless Personal Communications*, vol. 43, no. 2, pp. 389-409, Oct 2007.

[13] J. Fuhl, J.-P. Rossi, and E. Bonek, "High-resolution 3-D direction of arrival determination for urban mobile radio," *IEEE Transactions on Antennas and Propagation*, vol. 45, no. 4, pp. 672–682, Apr 1997.

[14] K. Kalliola, K. Sulonen, H. Laitinen, O. Kivelas, J. Krogerus, and P. Vainikainen, "Angular power distribution and mean effective gain of mobile antenna in different propagation environments," *IEEE Trans. Veh. Technol*, vol. 51, no. 5, pp. 823–838, Dec 2002.

[15] D. G. Valchev and D. Brady, "Three-dimensional multipath shape factors for spatial modeling of wireless channels," *IEEE Transactions on Wireless Communications*, vol. 8, no. 11, pp. 5542-5551, Nov 2009.

[16] S. M. Gulfam, S. J. Nawaz, A. Ahmed, and M. N. Patwary, "Analysis on multipath shape factors of air-to-ground radio communication channels," in *Proc. IEEE Wireless Telecommunications Symposium (WTS)*, 2016: 1-5.

[17] Yunlong Yu, Le Ru, and Kun Fang, "Bio-Inspired Mobility Prediction Clustering Algorithm for Ad Hoc UAV Networks," *Engineering Letters*, vol. 24, no. 3, pp. 328-337, 2016.
[18] Y. Fayad, C. Wang, and Q. Cao, "A Developed ESPRIT for Moving Target 2D-DOAE," *Engineering Letters*, vol. 24, no. 1, pp. 30-37, 2016.
[19] W. W. Bell, *Special Functions for Scientists and Engineers*. Dover Publications, Jul 2004.
[20] Y. Chen, L. Mucchi, R. Wang, and K. Huang, "Modeling Network Interference in the Angular Domain: Interference Azimuth Spectrum," *IEEE Transactions on Communications*, vol. 62, no. 6, pp. 2107-2120, Jun 2014.
[21] G. Alyami and I. Kostanic, "A Low Complexity User Selection Scheme with Linear Precoding for Massive MIMO Systems," *IAENG International Journal of Computer Science*, vol. 43, no. 3, pp. 374-379, 2016.
[22] N. C. Beaulieu and X. Dong, "Level crossing rate and average fade duration of MRC and EGC diversity in Ricean fading," *IEEE transactions on communications*, vol. 51, no. 5, pp. 722-726, May 2003.
[23] H. J. An, J. H. Kim, and H. K. Song, "Cooperative Transmission Scheme to Increase Gain by Using STBC," *Engineering Letters*, vol. 15, no. 1, pp. 135-139, 2007.

**Derong Du** received the B.E. degree in automation from the Chengdu University, Chengdu, China, in 2010 and the M.S. degree in control theory and control engineering from Guilin University of Electronic Technology, Guilin, China, in 2013. He is currently working towards the Ph.D. degree with the College of Communication Engineering, Chongqing University, Chongqing, China.

His research interests include the mobile radio channel modeling, multiple-input–multiple-output systems, vehicle-to-vehicle communications, and space information network.

**Xiaoping Zeng** received the B.E., M.S., and Ph.D. degrees in Electrical Engineering from Chongqing University, Chongqing, China in 1982, 1987, and 1996, respectively. He is now a professor and Ph.D. supervisor with the College of Communication Engineering, Chongqing University, China.

His research interests include the aeronautical information network, multiple-input–multiple-output systems, and the next generation mobile communication.

**Xin Jian** received his B.E. and Ph.D. degree from Chongqing University, Chongqing, China in 2009 and 2014, respectively. He is currently an associate professor with the College of Communication Engineering, Chongqing University, China.

His interests include multiple-input-multiple-output systems, vehicle-to-vehicle communications, and the next generation mobile communication.

**Feng Yu** received the B.E. degree in communication engineering from Wuhan University, Wuhan, China, in 2016. She is currently working toward the M.S. degree with the College of Communication Engineering, Chongqing University, Chongqing, China.

Her research interests include mobile radio channel modeling and the next generation mobile communication.

**Xiaoheng Tan** received the B.S. degree in radio communication engineering from Chongqing University, Chongqing, in 1998, and the Ph.D. degree in communication engineering from Chongqing University, in 2003. He is currently a professor and Ph.D. supervisor with the College of Communication Engineering, Chongqing University.

His research interests include the modern communication technology, broadband wireless access technology, and adaptive signal processing.

**Xin Jiang** received the Ph.D. degree from Beihang University (BUAA), Beijing, China. He is currently a research fellow and director of Avionics Department of Beijing Aeronautical Science & Technology Research Institute (BASTRI), a branch center of Commercial Aircraft Corporation of China (COMAC).

His research interests include internet of vehicles, general design of avionics systems, and airborne system technology.

**Wei Fang** received the Ph.D. degree in signal and information processing from Tianjin University, Tianjin, China, in 2013. He is currently a senior engineer of Beijing Aeronautical Science & Technology Research Institute (BASTRI), a branch center of Commercial Aircraft Corporation of China (COMAC).

His research interests include internet of vehicles, avionics systems, and aeronautical broadband communications.